

Frustrated three-leg spin tubes: from spin 1/2 with chirality to spin 3/2

J.-B. Fouet,¹ A. Läuchli,¹ S. Pilgram,² R. M. Noack,³ and F. Mila⁴

¹*Institut Romand de Recherche Numérique en Physique des Matériaux (IRRMA), CH-1015 Lausanne, Switzerland*

²*Theoretische Physik, ETH Zürich, CH-8098 Zürich, Switzerland*

³*Fachbereich Physik, Philipps Universität Marburg, D-35032 Marburg, Germany*

⁴*Institute of Theoretical Physics, Ecole Polytechnique Fédérale de Lausanne, CH-1015 Lausanne, Switzerland*

(Dated: December 2, 2024)

Motivated by the recent discovery of the spin tube $[(\text{CuCl}_2\text{tachH})_3\text{Cl}]\text{Cl}_2$, we investigate the properties of a frustrated three-leg spin tube with antiferromagnetic intra-ring and inter-ring couplings. We pay special attention to the evolution of the properties from weak to strong inter-ring coupling and show on the basis of extensive density matrix renormalization group and exact diagonalization calculations that the system undergoes a first-order phase transition between a dimerized gapped phase at weak coupling that can be described by the usual spin-chirality model and a gapless critical phase at strong coupling that can be described by an effective spin-3/2 model. We also show that there is a magnetization plateau at 1/3 in the gapped phase and slightly beyond. The implications for $[(\text{CuCl}_2\text{tachH})_3\text{Cl}]\text{Cl}_2$ are discussed, with the conclusion that this system behaves essentially as a spin-3/2 chain.

PACS numbers: 75.10.Dg, 75.60.Ej

I. INTRODUCTION

During the last fifteen years, spin ladders have attracted a lot of attention both from theoretical and experimental physicists (for an early review, see Ref. [1]). On one hand, they provide a calculationally tractable system interpolating between one-dimensional and two-dimensional quantum spin physics. On the other hand, existing spin ladder compounds allow for a detailed comparison of theoretical predictions and experimental results. The interpolation between one and two dimensions is however not smooth: while ladders with an even number of legs N show a gapped spectrum for spin excitations, ladders with odd N are believed to be gapless (like the spin-1/2 Heisenberg chain).

For odd N -ladders, applying periodic boundary conditions in the transverse direction of the ladder (forming thus a *spin tube*) yields an even more intriguing situation: In this case, for antiferromagnetic couplings, the ground state of an isolated ring is fourfold degenerate (twofold in spin- and twofold in chirality-space) and the low-energy physics of weakly coupled rings therefore involves both spin and chirality degrees of freedom. A number of theoretical studies have investigated effective low-energy Hamiltonians for weakly coupled rings by means of bosonization^{2,3}, density matrix renormalization group (DMRG)^{4,5}, mean field theory⁶, and exact diagonalization (ED)⁵. All of them conclude that the ground state is dimerized, displaying a gap for both spin and chirality excitations. The details of the gaps depend however on the frustration of the inter-ring coupling⁵.

Two experimental candidates for spin tubes are currently available: The vanadium oxide $\text{Na}_2\text{V}_3\text{O}_7$ ^{7,8,9}, probably a nine-leg spin tube but with only three-fold rotational symmetry, and the three-leg compound $[(\text{CuCl}_2\text{tachH})_3\text{Cl}]\text{Cl}_2$ ^{10,11}. None of these examples is in the regime of weak coupling between the rings, intra- and

inter-ring coupling constants being of the same order. It is therefore a very important first question to ask whether the low-energy physics of these realistic spin tubes may still be described by the above mentioned spin-chirality models. In both experimental realizations, neighboring rings are not coupled by one single antiferromagnetic bond, but by at least two competing bonds. This leads to additional frustration and raises the second question as to how much this frustration can change the physics.

We address both questions by considering the example of a three-leg tube with antiferromagnetic intra-ring couplings and two frustrating antiferromagnetic inter-ring couplings which forms a minimal setup including chirality and additional frustration. This model represents directly the compound $[(\text{CuCl}_2\text{tachH})_3\text{Cl}]\text{Cl}_2$, but the main results are expected to apply to other frustrated spin tubes as well. Regarding the properties, we will concentrate on the presence or absence of a spin gap, on the nature of the low-lying excitations, and on the magnetization curve.

The paper is organized as follows: In Sec. II we introduce the basic notations and describe several limiting cases of the three-leg spin tube. In Sec. III we discuss the zero-field phase diagram from a numerical point of view and report on low-spin boundary excitations. In Sec. IV we use continuous unitary transformations to derive effective low-energy Hamiltonians. Finally, we analyze the phase diagram as a function of the external magnetic field in Sec. V and discuss the experimental implications of our results in Sec. VI.

II. THE MODEL

The starting point is the Hamiltonian of the frustrated antiferromagnetic spin-1/2 Heisenberg model on a three-

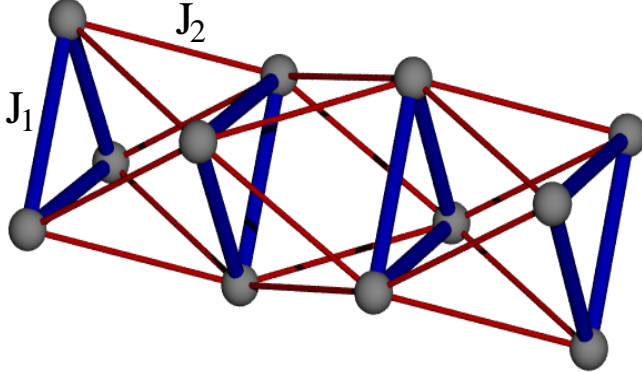


FIG. 1: (Color on-line) Three-leg spin tube with ring coupling J_1 (thick lines) and cross coupling J_2 (thin lines). Both couplings are antiferromagnetic, leading to frustration both *inside* the triangles and *between* the triangles.

leg spin tube:

$$H = J_1 \sum_{ij} \sigma_{ij} \cdot \sigma_{ij+1} + J_2 \sum_{ij} \sigma_{ij} \cdot (\sigma_{i+1j+1} + \sigma_{i+1j-1}). \quad (1)$$

The index i runs along the tube, $j = 1 \dots 3$ around the tube. The tube can be viewed as series of triangles (see Fig. 1). Each corner of such a triangle is coupled to two corners on the previous and the next triangle. In the absence of the J_1 coupling, the Hamiltonian is bipartite (see Fig. 1), and can be seen as a particular wrapping of a square lattice onto the tube.

A. Lieb Schultz Mattis Theorem

The Lieb Schultz Mattis (LSM) theorem¹² is one of the few exact results on frustrated spin systems. Since its proof is quite general, it can be applied to a wide variety of systems with short-range interaction^{13,14}, in particular, to the spin tube Hamiltonian (1). An explicit proof of the LSM theorem for this case can be found in Ref. [15]. The theorem states that half-integer spin chains have either a degenerate ground state or a gapless spectrum due to a zero-energy mode with momentum π relative to the ground state. It is interesting to note that both situations are realized in the three-leg spin tube system. We first discuss them in two limiting cases.

B. Weakly coupled triangles

In the limit $J_1 \gg J_2$, the system consists of weakly interacting triangles. Each isolated triangle has a four-fold degenerate spin-1/2 ground state that can be labeled by its chirality, τ_z , and its magnetic moment along the z axis, S_z . The projection of the full Hamiltonian (1) onto the low-energy space spanned by the spin-1/2 states leads

to lowest order in J_2 to an effective spin-chirality model,

$$\begin{aligned} H_{1/2} &= P_{S=1/2} H P_{S=1/2} \\ &\approx \frac{2J_2}{3} \sum_i \mathbf{S}_i \cdot \mathbf{S}_{i+1} (1 + \alpha [\tau_i^+ \cdot \tau_{i+1}^- + \text{h.c.}]) , \end{aligned} \quad (2)$$

where $\alpha = 2$ for the frustrated tube of Eq. (1). Here, \mathbf{S}_i is a spin-1/2 operator describing the total spin on triangle i , while τ_i is a pseudo-spin-1/2 operator acting in chirality space. The projector on the $S = 1/2$ subspace can be written as the product of the local projectors: $P_{S=1/2} = \prod_i P_{S=1/2}^i$, with:

$$P_{S=1/2}^i = \frac{15 - 4\mathbf{S}_i^2}{12} \quad (3)$$

The reduced spin-chirality Hamiltonian (2) has been studied in Ref. [5]. For $\alpha = 2$, it displays a dimerized ground state with a twofold degeneracy and gaps for both spin and chirality excitations.

C. Strongly coupled triangles

In the limit $J_1 = 0$, the lattice is effectively bipartite, and we expect ferromagnetic correlations between spins on the same ring because they belong to the same sublattice. The total spin on each ring should therefore be close to its maximum value of 3/2, and the physics for $J_1 = 0$ should be similar to the case of a ferromagnetic coupling, $J_1 < 0$, within each triangle. The effective Hamiltonian in the strong coupling case $-J_1 \gg J_2$ reads:

$$H_{3/2} = K_1 \sum_i \mathbf{S}_i \cdot \mathbf{S}_{i+1} + K_2 \sum_i (\mathbf{S}_i \cdot \mathbf{S}_{i+1})^2 . \quad (4)$$

where \mathbf{S}_i is now a spin-3/2 operator. The coupling constants are given by $K_1 = 2J_2/3 + J_2^2/(18|J_1|)$ and $K_2 = -J_2^2/(54|J_1|)$. Note that the nature of the second order corrections to K_1 and K_2 does not seem to frustrate the effective spin-3/2 chain. It is therefore reasonable to argue that the spin-3/2 state is stabilized at least up to $J_1 = 0$ even though this value lies beyond the perturbative limit. This argument can be made more quantitative by performing range-two CORE-calculations^{16,17} yielding effective coupling constants $K_1 = 0.70$ and $K_2 = 0.02$ for $J_1 = 0$. The physics of the effective Hamiltonian (4) is dominated by the Heisenberg (K_1) term, which is known to belong to the universality class of a Luttinger liquid¹⁸, and therefore has a gapless spectrum. Note that this is in sharp contrast to the gapped spectrum of the spin-chirality Hamiltonian (2).

Based on the preliminary arguments of subsections II B and II C, we expect the frustrated spin-tube Hamiltonian (1) to undergo at least one quantum phase transition as we move from weakly coupled ($J_1 \gg J_2$) to strongly coupled ($J_1 \ll J_2$) triangles.

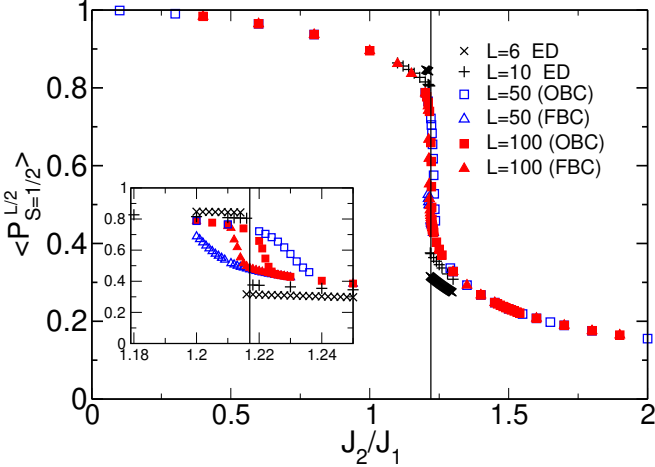


FIG. 2: (Color on-line) Expectation value of the projector $P_{S=1/2}^{L/2}$ in the bulk as a function of J_2/J_1 for different lengths and boundary conditions (see text). The jump at $J_2/J_1 \approx 1.22$ is a clear indication of a first-order transition.

III. NUMERICAL RESULTS

In the following, we investigate the properties of this phase transition numerically. We have performed extensive density matrix renormalization group (DMRG) calculations¹⁹ on tubes with open boundaries and $L \leq 100$ and exact diagonalization (ED) on small systems up to $L = 12$ using periodic boundary conditions (PBC).

Two independent quantities prove clearly that there is a single first-order bulk phase transition. They are discussed in Secs. III A and III B respectively. Furthermore, on open boundary systems, there is second “transition” at which the state of rings at the boundary jump from predominantly $S = 1/2$ to predominantly $S = 3/2$. This phenomenon will be discussed in Sec. III C.

A. Local spin on a ring

The first-order character is best seen in the ground state expectation value $\langle P_{S=1/2}^i \rangle$ of the previously defined projector (3), which is a purely local quantity defined on a single triangle i^{20} . We have computed this expectation value as a function of J_2 . The results are shown in Fig. 2, which displays the projector in the middle of the tube at $i = L/2$. For weak coupling, $J_2/J_1 \ll 1$, the expectation value is close to one, for strong coupling, $J_2/J_1 \gg 1$, it is close to zero. The expectation value clearly jumps at a value $J_{2c} = 1.219 \pm 0.003 J_1$ indicating a first-order phase transition which is magnified in the inset of Fig. 2.

Several comments are in order: Fig. 2 displays results obtained both with DMRG and ED. To check the importance of boundary effects (see Sec. III C), DMRG was performed with two types of boundary conditions: the standard Open Boundary Conditions (OBC), and the Ferromagnetic Boundary Conditions (FBC), where we

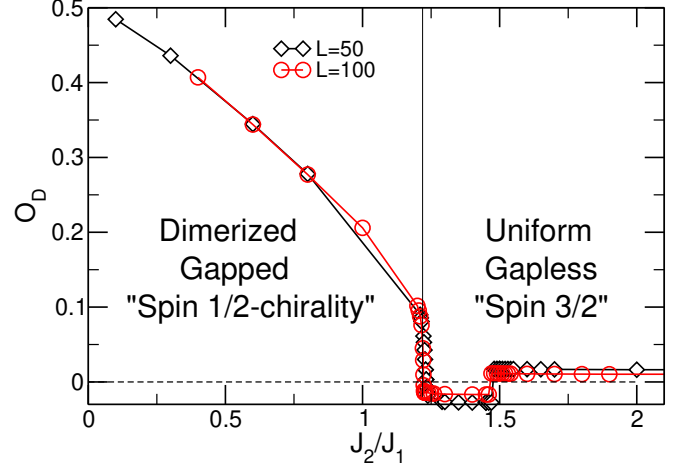


FIG. 3: (Color on-line) Dimerization at the center of the tube O_D as a function of J_2/J_1 for $L = 50$ (black squares) and $L = 100$ (red circles). The vertical line represents the disappearance of the true order parameter: The dimerization above this line vanishes after proper finite-size scaling.

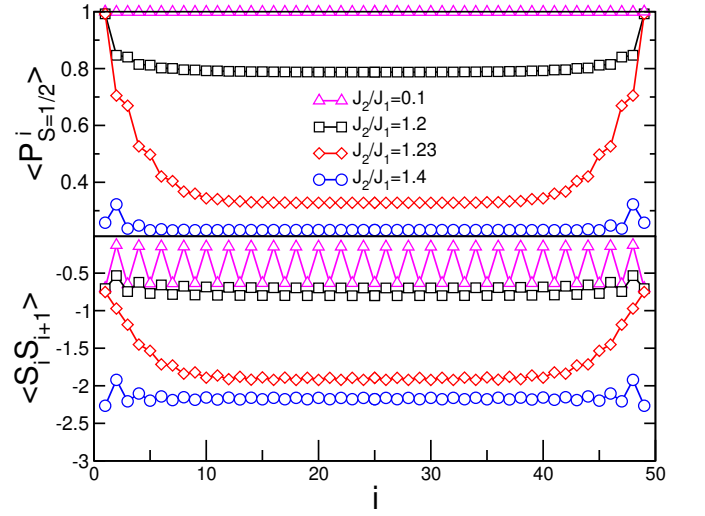


FIG. 4: (Color on-line) Spatial dependence of the projector $\langle P_{S=1/2}^i \rangle$ (upper panel) and nearest-neighbor correlation function $\langle \mathbf{S}_i \cdot \mathbf{S}_{i+1} \rangle$ (lower panel) for $L = 50$ and different values of the inter-ring coupling J_2 .

put a ferromagnetic coupling $J_1 = -10$ on the two triangles at the boundary of the tube, to force them to be into a $S = 3/2$ state. For the ED results, periodic boundary conditions were applied. The curves for the three kinds of boundary conditions differ only near the first-order transition, and the differences decrease with the increasing length of the tube. In the ED, we additionally observe that for system sizes $L = 4p + 2$ the ground state changes the momentum sector at the transition from $k = 0$ for weak coupling to $k = \pi$ for strong coupling. This is another fingerprint of a first-order transition.

B. Dimerization

The first-order character of the phase transition is also clearly apparent in inter-ring correlations. As an example, we investigate the local dimerization defined as

$$D_i = (-1)^i (\mathbf{S}_i \cdot \mathbf{S}_{i+1} - \mathbf{S}_{i+1} \cdot \mathbf{S}_{i+2}).$$

This dimerization can be viewed as the order parameter of the symmetry-broken weak coupling phase. It is also present in the spin-chirality model discussed in Sec. II B for which the dimerization opens a spin gap^{4,5,6}. Since we work with open boundary conditions, the quantity D_i varies with the ring position i . Fig. 3 shows the order parameter $O_D(L) = \langle D_{L/2} \rangle$ (the dimerization in the middle of the tube) for different system sizes L . Two sharp transitions are observed, the first one around $J_2 = J_{2c}$ and the second one at a higher value $J_2/J_1 \approx 1.47$. However, finite-size scaling shows that the order parameter $O_D(L)$ remains finite only for $J_2 < J_{2c}$ in the thermodynamic limit. The first transition, the disappearance of the dimerization, corresponds to the phase transition to a $S = 3/2$ phase on the rings. The second transition is a boundary effect discussed in the next section.

C. Boundary excitations

Boundary spin-1/2 degrees of freedom in open spin $S = 3/2$ chains have been predicted theoretically in Ref. [21], and were later confirmed in DMRG studies of unfrustrated²² and frustrated²³ spin $S = 3/2$ chains.

In our model we find these edge states as well for sufficiently large J_2/J_1 . However approaching the first-order transition coming from $J_2 > J_{2c}$, there is a second class of edge states, which are related to a kind of nucleation of the dimerized $S = 1/2$ phase at the boundaries. These edge states are different than those discussed above, as they now originate from the $S = 1/2$ subspace of a ring, and therefore also include a chirality degree of freedom.

This is most clearly seen in the spatial dependence of the correlation functions considered in the two subsections above. For different values of J_2/J_1 , the upper panel of Fig. 4 shows the space dependence of the projector $\langle P_{S=1/2}^i \rangle$ and the lower panel of the nearest-neighbor spin correlation $\langle \mathbf{S}_i \cdot \mathbf{S}_{i+1} \rangle$. The ring at the boundary stays in a predominant $S = 1/2$ state even for $J_2 > J_{2c}$, where the bulk transition has already occurred. The boundary spin-1/2 states disappear only beyond $J_2 \approx 1.5$. The nearest-neighbor spin-spin correlation function follows a similar behavior: the correlations at the boundary are close to those obtained in the bulk $S = 1/2$ phase, and then gradually approach the values of the bulk $S = 3/2$ phase.

The different behavior of bulk and edge rings are nicely illustrated in Fig. 5, in which the values of $\langle P_{(S=1/2)}^i \rangle$ in the bulk and at the boundary of the tube are plotted as a function of the coupling ratio J_2/J_1 . The expectation

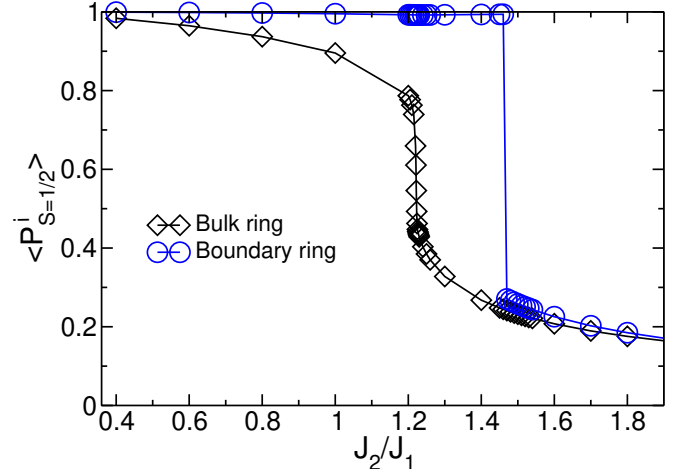


FIG. 5: (Color on-line) The projector $\langle P_{S=1/2}^i \rangle$ in the bulk and at the boundary of the tube for $L = 100$ jumps for different critical couplings indicating the existence of a boundary excitation.

value of the projector drops at $J_2/J_1 \approx 1.22$, whereas the boundary ring remains in a $S = 1/2$ state up to $J_2/J_1 \approx 1.5$.

IV. EFFECTIVE HAMILTONIAN APPROACH

After this numerical study, we now continue to analyze the properties of the effective low-energy Hamiltonians. We have previously discussed that the ground state of the model Hamiltonian (1) lies in the spin-1/2 sector for $J_1 \gg J_2$ and in the spin-3/2 sector for $J_2 \ll J_1$. The problem is then reduced to diagonalizing an effective Hamiltonian (2) or (4) on a truncated Hilbert space (for the spin-1/2 case see Refs. [4,5]). In the intermediate regime $J_1 \sim J_2$ the Hamiltonian mixes both sectors and such a truncation seems no longer possible. It is, however, interesting to observe that the above Hamiltonian H can be extended to

$$H_e = H + J'_2 \sum_{ij} \sigma_{ij} \cdot \sigma_{i+1j}.$$

For $J_2 = J'_2$, the extended H_e has the special property that the total spin and chirality of each triangle is conserved separately²⁴. In this case, it is again possible to find the ground state either in the truncated Hilbert space of the spin-1/2 sector or the spin-3/2 sector. This property is independent of the relative strength of J_1 and J_2 .

In the following, we construct an effective Hamiltonian H_{eff} which conserves the total number of spin-1/2 triangles in the system. The applied method can be viewed as an expansion in the perturbative parameter $J_2 - J'_2$. The obtained effective Hamiltonian allows us to calculate the ground state energies of the spin-1/2 and spin-3/2 sector

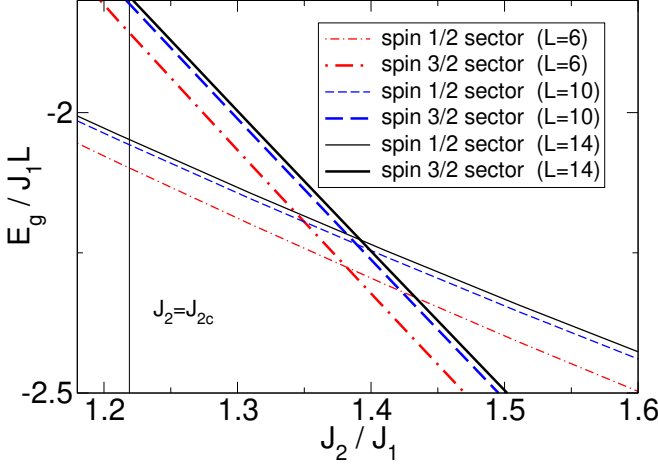


FIG. 6: (Color on-line) Comparison of ground state energies in the spin-1/2 and spin-3/2 sectors as a function of J_2/J_1 . Finite-size effects only appear for short tubes of length $N = 6, 8$. The first-order phase transition is located near $J_2 = 1.4J_1$. The discrepancy with the full numerical result is due to the truncation in the space of possible couplings.

independently, and to infer the critical J_2/J_1 by comparison of those energies.

A powerful tool for the derivation of effective Hamiltonians was introduced by Wegner²⁵, the so-called flow equations which were first applied to spin Hamiltonians by Uhrig²⁶. Flow equations apply infinitesimal unitary transformations to the original Hamiltonian until an effective Hamiltonian with the desired properties is obtained

$$\frac{dH(\ell)}{d\ell} = [\eta(\ell), H(\ell)], \quad H(\ell \rightarrow \infty) \rightarrow H_{\text{eff}}.$$

Following Ref. [25], we choose the commutator

$$\eta(\ell) = [H_c(\ell), H(\ell)]$$

as an appropriate generator of the transformation. Here, $H_c(\ell)$ denotes the conserving part of the Hamiltonian which does not change the number of spin-1/2 triangles.

As a first approximation, we decompose the Hamiltonian into a set of three couplings

$$H(\ell) = J_1(\ell)h_1 + J_{2,c}(\ell)h_{2,c} + J_{2,n}(\ell)h_{2,n}$$

and neglect all other types of couplings that are generated during the flow. Here, $h_{2,c}$ is the conserving part of the inter-triangle coupling h_2 which is readily obtained by applying the projectors (3) to h_2 . Analogously, $h_{2,n} = h_2 - h_{2,c}$ is the non-conserving part of the inter-triangle coupling. In this manner, we obtain three coupled differential equations for the coupling constants

$$\frac{dJ_1}{d\ell} = \left(32J_1 - 21\frac{1}{3}J_{2,c} \right) (J_{2,n})^2,$$

$$\frac{dJ_{2,c}}{d\ell} = \left(-13\frac{5}{7}J_1 + 19\frac{19}{63}J_{2,c} \right) (J_{2,n})^2,$$

and

$$\frac{dJ_{2,n}}{d\ell} = \left(-72J_1^2 + 96J_1J_{2,c} - 67\frac{5}{9}J_{2,c}^2 \right) J_{2,n}, \quad (5)$$

with the initial conditions

$$J_1(0) = J_1, J_{2,c}(0) = J_{2,n}(0) = J_2.$$

One easily checks that the quantity in brackets in the last equation is always negative, i.e., $J_{2,n}$ scales to zero during the flow, leading to an effective Hamiltonian of the desired form. Furthermore, for sufficiently large $J_2 > 3J_1/2$, we observe that $J_1(\ell)$ is monotonically decreasing along the flow whereas $J_{2,c}(\ell)$ is increasing.

The coupling $h_{2,c}$ obviously favors the triangles to be in a spin-3/2 state which can be better polarized by the antiferromagnetic coupling $h_{2,c}$. The flow equations (5) do not counteract this tendency, but even enhance it for sufficiently large J_2 since $J_{2,c}(\infty) > J_2$. For very large J_2 the effective $J_1(\infty)$ becomes ferromagnetic $J_1(\infty) < 0$, so that the one-site coupling h_1 itself favors the spin-3/2 state.

The accuracy of the above reasoning can be made semi-quantitative. For this purpose we evolve the one-site coupling and all the fifteen two-site nearest-neighbor couplings which are allowed by symmetry under the flow and evaluate the ground state energies in the spin-1/2 and spin-3/2 sectors by exact diagonalization of small tubes up to length $L = 14$. (Note that the dimension of the effective Hilbert space is reduced in comparison to the full Hilbert space by a factor of 2^L). The results of the numerical calculation are shown in Fig 6. The phase transition between a spin-1/2-chirality chain and a spin-3/2 chain appears around $J_2 \approx 1.4J_1$. This value lies slightly above the precise J_{2c} obtained by DMRG. As can be seen from Fig. 6, finite-size effects do not explain this quantitative discrepancy. It is in fact due to the truncation of the flow equations to nearest-neighbor couplings.

It can be checked numerically that the effect of including next-nearest neighbor two-site couplings in the flow is negligible. To reach a more quantitative result, it is necessary to include three-site couplings. These results will be presented elsewhere.

V. PHASE DIAGRAM IN A FIELD

In this section, we investigate the properties of the model in the presence of an external magnetic field.

For $J_2/J_1 = 0$, the triangles are decoupled and we expect a magnetization jump from $m = 0$ to $m = 1/3$ at $h = 0^+$, where all the triangles are in a spin-1/2 state with $S_z = +1/2$. This $m = 1/3$ plateau should survive in a finite parameter range. In terms of the spin-chirality model of Ref. [5], such a plateau is quite unusual. Indeed, when the spin degrees of freedom align ferromagnetically in the field, the effective model for the chirality becomes

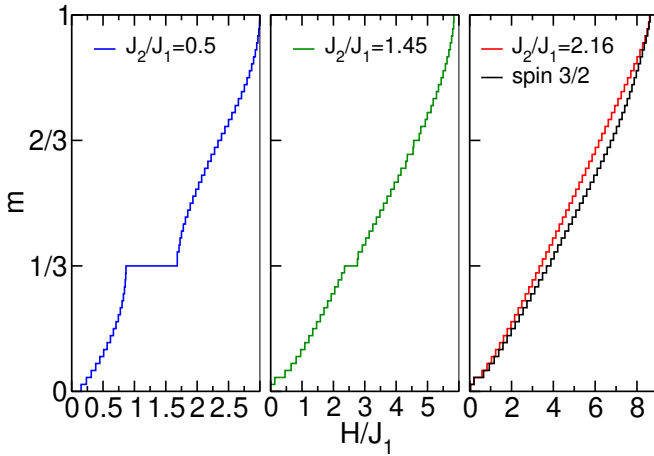


FIG. 7: (Color on-line) Magnetization curves for a spin tube with $L = 36$ and three different values of J_2/J_1 . In the right panel, we also show the magnetization curve of a $S = 3/2$ chain for comparison.

an XY model, whose spectrum is gapless. So, according to this argument, this plateau phase is expected to have a gap to spin excitations – as do all plateau phases – and to simultaneously possess gapless chirality excitations. Note that higher-order terms in the effective model might open a small gap in the chirality excitations as well, but being a higher order effect, this gap (if any) should be small compared to the spin gap, and should thus lead to observable properties, such as a specific heat linear in T below the temperature scale set by the width of the plateau.

Typical magnetization curves are shown in Fig. 7 for several values of J_2/J_1 . As long as the ratio J_2/J_1 is not too large, a plateau at $m = 1/3$ is clearly present. As can be seen in Fig. 8, this plateau phase survives everywhere in the region in which the system is effectively a spin-1/2 chain with chirality, but interestingly, it extends beyond that point up to $J_2/J_1 \approx 1.6$. It is plausible that the region of validity of the effective spin-1/2-chirality model extends to higher values of J_2/J_1 when a magnetic field is applied to the system. Indeed, an abrupt jump in $P_{S=1/2}^{L/2}$ is still present for slightly polarized samples and the corresponding critical value of the ratio J_2/J_1 increases slightly with magnetization. By the time the $m = 1/3$ plateau is reached, the suppression of $P_{S=1/2}^{L/2}$ is very smooth, however, and it is not possible to decide on the basis of the available data whether the first-order line extends up to the right boundary of the plateau phase, or whether it ends at a critical point on the way. In any case, for large J_2/J_1 , the magnetization curve becomes smooth, as it should for a spin-3/2 chain.

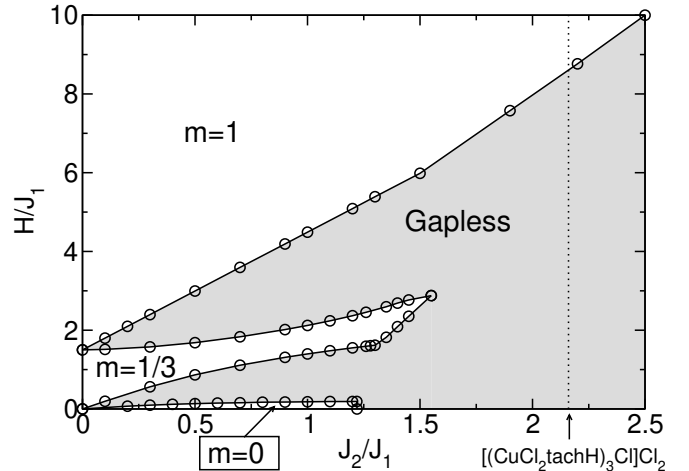


FIG. 8: Phase diagram as a function of J_2/J_1 and of the magnetic field H . Symbols are numerical data and solid lines are guides to the eye for the boundaries of the phase transitions. The gray area is a gapless phase, and the white area are plateau phases with a spin gap. Dotted line: experimental value of J_2/J_1 for the compound of Ref.[11]

VI. $[(\text{CuCl}_2\text{tachH})_3\text{Cl}]\text{Cl}_2$

The Hamiltonian of Eq. (1) is believed to be realized in the compound $[(\text{CuCl}_2\text{tachH})_3\text{Cl}]\text{Cl}_2$, with $J_2/J_1 \approx 2.16$, and the theoretical investigation of that model reported in Ref. [11] came to the somewhat surprising conclusion that the system has a gap to all (spin and singlet) excitations. This is at odds with the LSM theorem (see section II A). On the basis of our DMRG results, we do not reach the same conclusion. If J_2/J_1 is small enough, the system should be in a dimerized phase with a spin gap and a twofold degenerate groundstate. Hence a low-lying singlet excitation should be present in finite systems and should collapse onto the ground state in the thermodynamic limit. If J_2/J_1 is large enough, the system should essentially behave as a spin-3/2 chain and be gapless with low-lying spinon excitations. The phase transition between these phases takes place for $J_2/J_1 \approx 1.22$. So, with a ratio $J_2/J_1 \approx 2.16$, as deduced from the temperature dependence of the susceptibility in Ref. [11], we predict that $[(\text{CuCl}_2\text{tachH})_3\text{Cl}]\text{Cl}_2$ should have a gapless spectrum, and, since this ratio is also larger than the critical value that marks the disappearance of the 1/3 plateau, there should be no plateau at 1/3. In fact, according to the discussion of the previous section, the absence of a 1/3 plateau in the magnetization curve of $[(\text{CuCl}_2\text{tachH})_3\text{Cl}]\text{Cl}_2$ reported in Ref. [11] shows unambiguously that this compound lies in the effective $S = 3/2$ strong coupling phase.

To be more specific, the claim regarding the absence of a spin gap is clearly supported by our calculations of the gap to $S = 2$ excitations (since we are working with open boundary conditions, the gap to $S = 1$ excitations is very small and corresponds to boundary excitations^{21,22}). In-

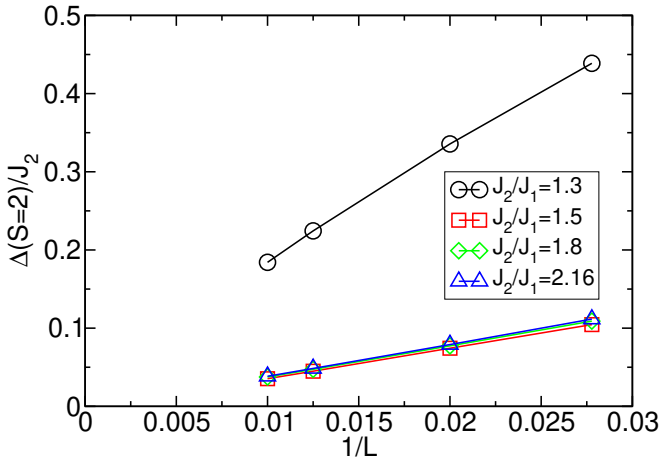


FIG. 9: (Color on-line) Gap to the $S=2$ sector (triangles) as a function of $1/L$ for several values of J_2/J_1

deed, the finite-size scaling of the gap is consistent with a vanishing value in the thermodynamic limit for all ratios J_2/J_1 larger than 1.22 (see Fig. 9).

Regarding the magnetization curve, our results agree with those of Ref. [11], which were obtained on smaller systems: The curve is smooth with no trace of any irregularity close to 1/3-magnetization. Fig. 7 shows the magnetization curve for the spin tube for various value of J_2 and for the spin-3/2 chain for $L = 36$. The coupling of the spin-3/2 chain has been chosen so that the saturation field is the same as the saturation field for the experimental value of the couplings ($J_2/J_1 = 2.16$). The two magnetization curves are very similar giving further support to our claim that $[(\text{CuCl}_2\text{tachH})_3\text{Cl}]\text{Cl}_2$ should be regarded as a spin-3/2 chain. It would be desirable to have additional low-temperature susceptibility data in order to clarify whether the compound really shows a spin gap. On the basis of the available susceptibility

and magnetization data, gapless behavior is clearly not excluded.

VII. CONCLUSIONS

We have investigated three-leg spin tubes consisting of rings that are coupled by competing antiferromagnetic bonds. We have shown that this frustration can drive the system away from the typically used effective spin-1/2-chirality model of regular spin tubes. It becomes an effective spin-3/2 chain even if the inter-ring couplings are antiferromagnetic. In the specific case of the model relevant to $[(\text{CuCl}_2\text{tachH})_3\text{Cl}]\text{Cl}_2$ in which each spin of a ring is coupled to two spins of the neighboring rings, the transition between these phases as a function of the inter-ring coupling has been shown to be first order. This should be contrasted to the case of the unfrustrated spin tube, in which case the transition is expected to be second order and to take place when the inter-ring coupling changes sign. These results lead to a new interpretation of the properties of $[(\text{CuCl}_2\text{tachH})_3\text{Cl}]\text{Cl}_2$, and to specific predictions regarding the occurrence of a plateau at 1/3 in this geometry. It is our hope that the present work will motivate further investigations of the excitations of $[(\text{CuCl}_2\text{tachH})_3\text{Cl}]\text{Cl}_2$ to check our predictions, and more generally of the (so far) small but fascinating family of spin tubes.

Acknowledgments

We are thankful to Sabrina Rabello, who was involved at an early stage of this project. This work was supported by the Swiss National Fund and by MaNEP. Calculations have been partly performed on the Pleiades cluster of EPFL.

¹ E. Dagotto and T. M. Rice, *Science* **271**, 618 (1996)

² H. J. Schulz, in “Correlated Fermions and Transport in Mesoscopic Systems”, ed. T. Martin, G. Montambaux, J. Tran Than Van (Editions Frontiers, Gif-sur-Yvette, 1996) p.81.

³ D. C. Cabra, A. Honecker, and P. Pujol, *Phys. Rev. B* **58**, 6241 (1998).

⁴ K. Kawano and M. Takahashi, *J. Phys. Soc. Jpn.* **66**, 4001 (1997).

⁵ A. Lüscher, R. M. Noack, G. Misguich, V. N. Kotov and F. Mila, *Phys. Rev. B* **70**, 060405(R) (2004).

⁶ H.-T. Wang, *Phys. Rev. B* **64**, 174410 (2001).

⁷ P. Millet, J. Y. Henry, F. Mila, and J. Galy, *J. Solid State Chem.* **147**, 676 (1999).

⁸ J. L. Gavilano, D. Rau, S. Mushkolaj, H. R. Ott, P. Millet, and F. Mila, *Phys. Rev. Lett.* **90**, 167202 (2003).

⁹ J. L. Gavilano, E. Felder, D. Rau, H. R. Ott, P. Millet, F. Mila, T. Cichorek, and A. C. Mota, *cond-mat/0501756* (2005).

¹⁰ G. Seeber, P. Kögerler, B. M. Kariuki, and L. Cronin, *Chem. Commun. (Cambridge)* **2004**, 1580 (2004).

¹¹ J. Schnack, H. Nojiri, P. Kögerler, G. T. Cooper and L. Cronin, *Phys. Rev. B* **70**, 174420 (2004).

¹² E. Lieb, T. Schultz, and D. Mattis, *Ann. Phys.(N.Y.)* **16**, 407 (1961)

¹³ I. Affleck *Phys. Rev. B* **37** 5186 (1988).

¹⁴ M. Oshikawa, M. Yamanaka, and I. Affleck *Phys. Rev. Lett.* **78** 1984 (1997).

¹⁵ A. G. Rojo, *Phys. Rev. B* **53**, 9172 (1996).

¹⁶ C.J. Morningstar and M. Weinstein, *Phys. Rev. D* **54** 4131 (1996).

¹⁷ S. Capponi, A. Läuchli and M. Mambrini, *Phys. Rev. B* **70**, 104424 (2004).

¹⁸ K. Hallberg, X.Q.G. Wang, P. Horsch, and A. Moreo, *Phys. Rev. Lett.* **76**, 4955 (1996).

¹⁹ S.R. White, *Phys. Rev. Lett.* **69**, 2863 (1992); *Phys. Rev.*

B **48**, 10 345 (1993).
²⁰ X. Wang, N. Zhu, and C. Chen Phys. Rev. B **66**, 172405 (2002).
²¹ T.K. Ng, Phys. Rev. B **50**, 555 (1994).
²² S. Qin, T. Ng, and Z. Su, Phys. Rev. B **52**, 12844 (1995).
²³ R. Roth and U. Schollwöck, Phys. Rev. B **58**, 9264 (1998).
²⁴ A. Honecker, F. Mila, and M. Troyer, Eur. Phys. J. **B15** 227 (2000).
²⁵ F. J. Wegner, Ann. Physik **3**, 77 (1994).
²⁶ G. S. Uhrig, Phys. Rev. B **57**, R14004 (1998).